AIP | The Journal of Chemical Physics

Crossing the dividing surface of transition state theory. III. Once and only once. Selecting reactive trajectories

J. C. Lorquet

Citation: The Journal of Chemical Physics **143**, 104314 (2015); doi: 10.1063/1.4930273
View online: http://dx.doi.org/10.1063/1.4930273
View Table of Contents: http://scitation.aip.org/content/aip/journal/jcp/143/10?ver=pdfcov
Published by the AIP Publishing

Crossing the dividing surface of transition state theory. III. Once and only once. Selecting reactive trajectories

J. C. Lorquet[a)]
Department of Chemistry, University of Liège, Sart-Tilman (Bâtiment B6), B-4000 Liège 1, Belgium

(Received 22 June 2015; accepted 26 August 2015; published online 14 September 2015)

The purpose of the present work is to determine initial conditions that generate reacting, recrossing-free trajectories that cross the conventional dividing surface of transition state theory (i.e., the plane in configuration space passing through a saddle point of the potential energy surface and perpendicular to the reaction coordinate) without ever returning to it. Local analytical equations of motion valid in the neighborhood of this planar surface have been derived as an expansion in Poisson brackets. We show that the mere presence of a saddle point implies that reactivity criteria can be quite simply formulated in terms of elements of this series, irrespective of the shape of the potential energy function. Some of these elements are demonstrated to be equal to a sum of squares and thus to be necessarily positive, which has a profound impact on the dynamics. The method is then applied to a three-dimensional model describing an atom-diatom interaction. A particular relation between initial conditions is shown to generate a bundle of reactive trajectories that form reactive cylinders (or conduits) in phase space. This relation considerably reduces the phase space volume of initial conditions that generate recrossing-free trajectories. Loci in phase space of reactive initial conditions are presented. Reactivity is influenced by symmetry, as shown by a comparative study of collinear and bent transition states. Finally, it is argued that the rules that have been derived to generate reactive trajectories in classical mechanics are also useful to build up a reactive wave packet. © *2015 AIP Publishing LLC*. [http://dx.doi.org/10.1063/1.4930273]

I. INTRODUCTION

In 1938, Wigner[1] developed a simple model based on the concept of a dividing surface in phase space, which formulated transition state theory (TST) in a general dynamical context and which laid the foundation for its success. This surface is defined as a partition separating reactants from products. The theory is most easily implemented if the dividing surface is reduced to a plane in configuration space, passing through a saddle point of the potential energy surface and perpendicular to the path of steepest descent. The direction normal to this plane is termed the reaction coordinate. Reactive trajectories are assumed to cross the dividing surface from reactant to product space without ever recrossing. This simple model provides the basis for chemical reactivity theories, but the recrossing problem is a major issue of concern.

To overcome the problem, several strategies have been adopted. Variational TST,[2] restricted to configuration space, provides a very popular method. However, a really satisfactory solution requires a reformulation of TST in phase space, as opposed to configuration space. Elegant solutions, unfortunately valid for two-dimensional systems only, have been developed by Pollak and Pechukas[3] and by Davis and Gray.[4]

However, it later on emerged that multidimensional dividing surfaces exist only in phase space, not in configuration space. The impetus was given by Miller who, in a seminal paper,[5] showed the dynamics near a saddle point to be integrable and proposed a way to calculate the reactive flux in the full phase space of a nonseparable system.[6,7] This breakthrough paved the way for a number of significant papers[8–15] aiming at developing rigorous methods to partition multidimensional phase space into reactant and product regions and at constructing hypersurfaces of no return in the phase space of strongly coupled, multidimensional systems. The dynamics that takes place in the neighborhood of a saddle is described in terms of so-called normal form coordinates, mixing spatial coordinates, and momenta, which reveal the presence of integrals of the motion. This procedure leads to the perturbative construction of phase space structures termed normally hyperbolic invariant manifolds. These elaborate mathematical concepts represent a major advance but are not yet part of the cultural stock in trade of chemists. Furthermore, their implementation requires heavy computational artillery.

Incidentally, this mathematical analysis reveals that TST is not confined to chemical reaction dynamics: the derived methods have found applications in a bewildering variety of topics ranging from electronics to astrophysics.[8,9,14]

The strategy adopted here starts from an analysis of the shortcomings of the conventional planar dividing surface in configuration space containing the saddle point and normal to the path of steepest descent, that is the basis of chemical intuition in reaction rate theory.

Previous research, published as Papers I and II of the present series,[16,17] has shown that, if the transition state (TS) is tight enough, more than one half of the trajectories have to be discarded as nonreactive, either because they rapidly recross this conventional surface or because they have previously done so at a short negative time. More specifically, one fourth of

a)Electronic mail: jc.lorquet@ulg.ac.be

them recross rapidly in a short period of time. Another fourth of them have their origin in the fragment space and recross at a short negative time before recrossing again for the last time at $t = 0$ and pursuing their course to infinity. Explicit analytical estimations of these recrossing times could be derived for these early recrossings. Furthermore, the remaining half is not at all free from recrossings: it can be expected to undergo an undetermined number of recrossings at longer (positive or negative) times. The conventional choice for the dividing surface thus appears particularly unfortunate and highly questionable, if not totally inadequate.[12,13,15]

Clearly, a change in strategy is required. In the present contribution, instead of trying to determine a recrossing-free dividing surface, we look for a way to select trajectories that do not recross the conventional surface. This means that the plane in configuration space containing the saddle point and perpendicular to the unstable vibrational mode is still considered. However, this plane is no longer seen as the dividing surface: it serves to define initial conditions that generate truly reactive trajectories.

In TST, the reactivity criterion is both unique and extremely simple: the momentum vector of the trajectory must have a component on the normal to the planar surface. This condition is obviously necessary, but not sufficient, and it is our wish to derive additional specifications.

In Sec. II, we present a method to derive local analytical equations of motion valid in the neighborhood of the planar surface as an expansion in Poisson brackets. We show that reactivity criteria can be quite simply formulated in terms of elements of this series, irrespective of the shape of the potential. The method is then applied in Sec. III to a three-dimensional model describing an atom-diatom interaction. A particular solution defining a so-called "central reactive trajectory" is examined in Sec. IV. This particular case is extended in Sec. V to define reactive cylinders in phase space. The validity of analytical reactivity criteria is checked by numerical classical trajectory calculations in Sec. VI. A general discussion is given in Sec. VII. The paper concludes with an excursion into the realm of quantum mechanics, which shows that the previous considerations should be useful to build up a reactive wave packet.

II. EQUATIONS OF MOTION

A. A formal series solution

A closed-form expression of Hamilton's canonical equations cannot be obtained in the neighborhood of the saddle point. However, a very general procedure to derive local analytic solutions in the form of a series expansion has been presented in Papers I and II.[16,17]

If X denotes a particular coordinate or momentum, it is possible to derive a solution of the corresponding differential equations of motion as a series expansion by repeated applications of the Poisson bracket equation,[18]

$$\dot{X} = [X,H] \equiv \sum_j \left(\frac{\partial H}{\partial p_j}\frac{\partial X}{\partial q_j} - \frac{\partial H}{\partial q_j}\frac{\partial X}{\partial p_j} \right), \qquad (2.1)$$

which gives the rate of change of any dynamical variable X.

We are particularly interested in the case $X = R$, where R denotes the reaction coordinate. Its equation of motion can be formulated as follows:[18]

$$\begin{aligned} R(t) &= R_0 + t[R,H]_0 + \left(\frac{t^2}{2!}\right)[[R,H],H]_0 \\ &\quad + \left(\frac{t^3}{3!}\right)[[[R,H],H],H]_0 + \cdots \\ &= R_0 + c_1 t + c_2\left(\frac{t^2}{2!}\right) + c_3\left(\frac{t^3}{3!}\right) + \cdots, \end{aligned} \qquad (2.2)$$

where the subscript zero refers to the initial conditions at time $t = 0$, defined as the time at which the surface is crossed.

B. Reactivity criteria

In order to derive reactivity criteria, we must find a way to select trajectories that cross the plane containing the saddle point once and only once. Consider first a one-dimensional motion: a particle flies over a parabolic potential energy barrier having its maximum at point $x = x_0$. The equation of motion is simple: $x(t) = x_0 + \sinh(\gamma t)$.

Extrapolating from this elementary case, it is easily understood that for more general potentials initial conditions should be chosen so that

(1) even-power coefficients (quadratic, quartic, ...) should be absent from the Taylor expansion of the actual equation of motion (i.e., from Eq. (2.2)) because these terms inflect the trajectory and induce recrossings at positive times (if $c_2 < 0$) or at negative times (if $c_2 > 0$).
(2) Odd-power coefficients (linear, cubic, quintic, ...) should all be positive (and as large as possible).

We now wish to substantiate these expectations by considering more realistic models. If the shape of the energy barrier is undetermined, except that it is known to have its maximum at point $x = x_0$, then Eq. (2.2) can be applied to the Hamiltonian $H(x,p_x) = {p_x}^2/2M + V(x)$. Nothing is assumed about $V(x)$, except two obvious properties: $V'(x_0) = 0$ and $V''(x_0) < 0$. This leads to the following result for odd-order coefficients:

$$c_{2j+1} = p_{x_0} M^{-j-1}(-V''(x_0))^j + \text{h.o.t.}, \qquad (2.3)$$

where the symbol h.o.t. denotes additional higher-order terms. Thus, odd-order coefficients are necessarily positive, as expected.

The higher-order terms are equal to zero for c_1 and c_3. For c_5, one has

$$c_5 = p_{x_0} M^{-3} V''(x_0)^2 - p_{x_0}^3 M^{-4} V^{(4)}(x_0), \qquad (2.4)$$

where the symbol $V^{(4)}$ denotes the fourth-order derivative of the potential.

The magnitude of these terms is essentially determined by the heaviness of the nuclear masses that appear in the denominators. In practice, Eq. (2.4) can be truncated after its first term. However, for high-order odd coefficients (c_9 and higher), the number and magnitude of high-order corrective terms increase rapidly, so that it becomes insecure to limit the expansion to its leading term. Furthermore, no information is known on the magnitude of high-order derivatives of the potential. This is as

it should be. The initial evolution is dictated by the properties of the maximum. But at a later stage, it depends on the presence of either a minimum or of an asymptotic levelling off.

The quadratic coefficient c_2, which determines the acceleration of the motion at $t = 0$, is equal to zero, as might have been expected. The leading term of higher-order even coefficients is given by

$$c_j = -k_j M^{-j/2-1} p_{x_0}^2 V^{(3)}(x_0) \left(-V''(x_0)\right)^{j/2-2}, \quad (2.5)$$

where k_j is a positive number for which no simple expression could be derived. Even-order terms can be expected to be small because of the presence of heavy nuclear masses in their denominator.

Similar calculations were carried out for two-dimensional Hamiltonians and similar conclusions were derived, but we shall not go into it. Instead, we go straight to the analysis of a more realistic three-dimensional model.

C. A particular solution for an arbitrary three-dimensional potential

Consider a dynamical system with three degrees of freedom studied in a body-fixed referential. The kinetic energy describing an atom-diatom interaction for a rotationless motion has been derived in Jacobi coordinates by several authors,[11,12,19,20]

$$H = \frac{1}{2M} P_R^2 + \frac{1}{2\mu} p_r^2 + \frac{1}{2}\left(\frac{1}{MR^2} + \frac{1}{\mu r^2}\right) p_\theta^2 + V(R, r, \theta), \quad (2.6)$$

where R is the distance between the atom and the center of mass of the diatomic, r the internuclear distance of the latter, θ the angle between the two position vectors, P_R, p_r, p_θ the conjugate momenta, μ the reduced mass of the diatomic, and M that of the atom-diatom system. The potential energy function is completely arbitrary, except that it is characterized by a saddle point at coordinates (R_*, r_*, θ_*). This implies conditions on its first and second derivatives,

$$\left.\frac{\partial V}{\partial R}\right|_* = \left.\frac{\partial V}{\partial r}\right|_* = \left.\frac{\partial V}{\partial \theta}\right|_* = 0, \quad (2.7)$$

$$\left.\frac{\partial^2 V}{\partial R^2}\right|_* < 0, \left.\frac{\partial^2 V}{\partial r^2}\right|_* > 0, \left.\frac{\partial^2 V}{\partial \theta^2}\right|_* > 0, \quad (2.8)$$

where the asterisk indicates that the expression is evaluated at the saddle point.

Our aim is the detection of mathematical properties of the nested structure of Poisson brackets that exist irrespective of the shape of the potential energy surface.

The linear coefficient in Eq. (2.1), namely, $c_1 = [R, H]_0 = P_{R*}/M$, is invariably chosen to be positive in TST. Here again, the subscript zero refers to the initial conditions at time $t = 0$, defined as the time at which the surface is crossed.

The second coefficient,

$$c_2 = [[R, H], H]_0 = \frac{P_{\theta_0}^2}{M^2 R_*^3} - \frac{1}{M}\left.\frac{\partial V}{\partial R}\right|_0, \quad (2.9)$$

measures the acceleration along the reaction coordinate. In order to determine a presumably reactive trajectory, we require this even-order coefficient to vanish. This happens if the various components compensate so that the total acceleration vanishes. However, this can also be done in a trivial way by starting the trajectory right at the saddle point, i.e., by adopting the following set of initial conditions:

$$R = R_*, P_R = P_{R_*} > 0, r = r_*, P_r, \theta = \theta_*, P_\theta = 0, \quad (2.10)$$

because all of the first derivatives of V vanish at that point. In addition, in order to dispose of the first term of the right-hand side of Eq. (2.9), we also require the angular momentum P_θ to vanish. As a result, the internal energy is then initially distributed between the translational and vibrational momenta.

The third coefficient, c_3, measures the rate of change of the acceleration. It is sometimes referred to as the jerk. When the set of initial conditions expressed in Eq. (2.10) is adopted, it is equal to the sum of two terms,

$$c_3 = -\frac{P_{R_*}}{M^2}\left.\frac{\partial^2 V}{\partial R^2}\right|_* - \frac{P_r}{M\mu}\left.\frac{\partial^2 V}{\partial R \partial r}\right|_*. \quad (2.11)$$

Initial conditions should be chosen to make it positive and as large as possible. Since the second derivative $\partial^2 V/\partial R^2|_*$ is necessarily negative at a saddle point, a high value of the initial translational momentum P_{R_*} is necessarily beneficial to reactivity. Energy flow into the vibrational momentum is helpful provided that the sign of P_r is properly chosen, namely, provided that

$$P_r \left.\frac{\partial^2 V}{\partial R \partial r}\right|_* < 0. \quad (2.12)$$

Still continuing to use the set of initial conditions given in Eq. (2.10), the expression of the quartic coefficient can be derived in a similar way,

$$c_4 = -\frac{P_{R_*}^2}{M^3}\left.\frac{\partial^3 V}{\partial R^3}\right|_* - 2\frac{P_{R_*} P_r}{M^2 \mu}\left.\frac{\partial^3 V}{\partial R^2 \partial r}\right|_* - \frac{P_r^2}{M\mu^2}\left.\frac{\partial^3 V}{\partial R \partial r^2}\right|_*. \quad (2.13)$$

The result is too complicated to derive detailed criteria. However, two findings emerge, which offer prospects for a small magnitude and a reduced influence of the quartic coefficient:

(1) Its M^{-3} dimensionality (compared with M^{-1} for c_1 and M^{-2} for c_2 and c_3).
(2) The potential energy function V is necessarily a very complicated function of the coordinates so that, once its expression is made explicit, the right hand side of Eq. (2.13) splits into such a large number of terms that statistical cancellation can be expected to operate.

We now turn to the expression of the quintic coefficient. Its leading term is

$$c_5 = \left(\frac{1}{M}\left(\left.\frac{\partial^2 V}{\partial R^2}\right|_*\right)^2 + \frac{1}{\mu}\left(\left.\frac{\partial^2 V}{\partial R \partial r}\right|_*\right)^2 + \frac{1}{I}\left(\left.\frac{\partial^2 V}{\partial R \partial \theta}\right|_*\right)^2\right)\frac{P_{R_*}}{M^2} + \left(\left.\frac{\partial^2 V}{\partial R \partial r}\right|_*\left(\frac{1}{M}\left.\frac{\partial^2 V}{\partial R^2}\right|_* + \frac{1}{\mu}\left.\frac{\partial^2 V}{\partial r^2}\right|_*\right) + \frac{1}{I_*}\left.\frac{\partial^2 V}{\partial R \partial \theta}\right|_*\left.\frac{\partial^2 V}{\partial r \partial \theta}\right|_*\right)\frac{P_r}{M\mu}, \quad (2.14)$$

where I_* denotes the reduced moment of inertia,

$$I_* = \left(\frac{1}{MR_*^2} + \frac{1}{\mu r_*^2}\right)^{-1}. \tag{2.15}$$

An important finding is that the coefficient of P_{R*} is a sum of squares and is thus necessarily positive. Therefore, a high value of the initial translational momentum is always beneficial to reactivity. Thus, irrespective of the expression of the potential energy function $V(R,r,\theta)$, energy flow into the reaction coordinate necessarily increases reactivity because it necessarily increases the magnitude of the odd-order coefficients (linear, cubic, and quintic) when initial conditions are chosen that reduce even-order coefficients to zero or to a small value.

The role of the vibrational momentum P_r cannot be ascertained because the sign of its coefficient in Eq. (2.14) cannot be determined *a priori*. However, there are reasons to believe that its role is less significant because at a saddle point the two curvatures $\partial^2V/\partial R^2\big|_*$ and $\partial^2V/\partial r^2\big|_*$ are necessarily opposite and might to some extent cancel each other.

Note in addition that, as shown by a comparison between Eqs. (2.11) and (2.14), the situation concerning the role of P_r is different for the cubic and quintic coefficients and may lead to contradictory requirements. In the former case, the propensity is quite simply expressed in Eq. (2.12), whereas it is more complicated and *a priori* undecidable in the latter.

The expression of high-order odd coefficients is too complicated to be reported here. For c_7, the translational momentum P_{R*} is multiplied by the sum of six terms, whose sign is positive for three of them, negative for two, and undecidable for the last one with a presumably small modulus. In the expression of c_9, the translational momentum P_{R*} is multiplied by the sum of 14 terms, ten of which necessarily positive, two necessarily negative, and two with an undecidable sign but presumably small modulus.

Thus, irrespective of the shape of the potential energy surface, the set of initial conditions defined in Eq. (2.10) determines a particular reactive trajectory. Starting the trajectory right at the saddle point with a zero value for P_θ trivially satisfies the zero-acceleration condition. Furthermore, the intuitively obvious fact that a high value of the initial translational momentum necessarily increases reactivity is given a mathematical rationalization: a high value of P_{R*} increases the magnitude of the linear, cubic, and quintic odd-order coefficients, and probably also higher-order ones, although this could be checked only up to c_9.

As a final general remark, we note that the accuracy of the series expansion considered in Eq. (2.2) is greatly helped not only by the factorials that appear in the denominators, but also by the heaviness of nuclear masses: Coefficients of order $(2N+1)$ or $2N$ have a dimension proportional to M^{-N-1} or M^{-N}, respectively, which means that they steadily decrease as N increases.

Summing up, the set of initial conditions defined in Eq. (2.10) generates a reactive trajectory. We refer to it as "the central reactive trajectory," because there is hope that "adjacent trajectories," where small but nonzero deviations are introduced into the initial values of r, θ, and P_θ, will also be reactive. This concept was initially introduced by Hutchinson and co-workers.[21] We note finally that it is strongly reminiscent of results derived by Wiggins and co-workers.[12] In their study of the isomerization of HCN, these authors define "dynamical reaction paths" by setting all coordinates other than those associated with the reaction coordinate to zero ("no energy in the bath modes"). There are two differences, though: (i) Jacobi coordinates have been transformed to the normal form; (ii) in our formulation, it is not necessary to set P_r to zero because the acceleration term c_2 is independent of it.

The question is now whether these rules also apply to adjacent trajectories.

III. A SPECIFIC HAMILTONIAN

In order to determine whether deviations from initial conditions expressed in Eq. (2.10) (i.e., nonzero extensions from the saddle point geometry together with nonzero rotational momentum) will also generate reactive trajectories, we consider a specific Hamiltonian designed to represent a typical potential energy surface presenting a saddle point of a type frequently encountered in molecular reaction dynamics. Specifically, the potential is written as a sum of two- and three-body contributions, adopting the simplest possible expression for the two-body terms and shifting most of the couplings to the three-body term,

$$V(R,r,\theta) = V_{saddle}(R) + V_{diat}(r,R) + V_{ang}(\theta,R) + V_{3b}(R,r,\theta). \tag{3.1}$$

This function has been described in detail in Paper II[17] and we recapitulate only its essential features.

The first term of this expansion, representing a cross-section along the reaction coordinate, is written as an inverted 6–12 Lennard-Jones potential where the zero of energy has been shifted to the saddle point,

$$V_{saddle}(R) = -\frac{MR_*^2\Omega^2}{72}\left(1 - \left(\frac{R_*}{R}\right)^6\right)^2, \tag{3.2}$$

where Ω denotes the modulus of an imaginary frequency which, as will be seen shortly, is not an observable but a zeroth-order quantity.

The next two-body term describes the vibrational motion of the diatomic fragment. To introduce anharmonicity in a simple way, a Simons-Parr-Finlan potential is used.[20,22] Furthermore, curvature of the reaction path is introduced by allowing the frequency and equilibrium distance of the diatomic fragment to depend on the reaction coordinate R. Altogether,

$$V_{diat}(r,R) = \frac{1}{2}\mu\omega(R)^2\big(r - r_{eq}(R)\big)^2\left(\frac{r_{eq}(R)}{r}\right)^2, \tag{3.3}$$

with

$$r_{eq}(R) = r_\infty + (r_* - r_\infty)\left(\frac{R_*}{R}\right)^6, \tag{3.4}$$

$$\omega(R) = \omega_\infty + (\omega_* - \omega_\infty)\left(\frac{R_*}{R}\right)^6, \tag{3.5}$$

where r_∞ and ω_∞ denote the equilibrium distance and angular frequency of the diatomic fragment after complete separation, respectively. The inverse sixth power dependence is in line

with the assumption of an inverse Lennard-Jones potential for the reaction coordinate.

Angles are measured so that the equilibrium value (denoted θ_* at the saddle point) is positive and tends to zero as R increases. The potential that determines the angular motion, which is a hindered rotation with a strongly R-dependent barrier, is written as

$$V_{ang}(\theta,R) = V_0\left(\frac{R_*}{R}\right)^6 \sin^2\left(\theta - \theta_{eq}(R)\right), \tag{3.6}$$

with

$$\theta_{eq}(R) = \theta_*\left(\frac{R_*}{R}\right)^6. \tag{3.7}$$

To derive the expression of the three-body interaction term, we adapt Murrell's procedure to a saddle point topography described in Jacobi coordinates.[23] As described in detail in Paper II,[17] we write

$$V_{3b}(R,r,\theta) = P_{3b}(R,r,\theta)\left(\frac{R_*}{R}\right)^6\left(1-\left(\frac{R_*}{R}\right)^6\right) \times\left(1-\tanh\left(\frac{\gamma}{2}\left(r-r_{eq}(R)\right)\right)\right), \tag{3.8}$$

with

$$P_{3b}(R,r,\theta) = \beta_{RR}(R-R_*)^2 + \beta_{rr}(r-r_*)^2 + \beta_{\theta\theta}(\theta-\theta_*)^2 + \beta_{Rr}(R-R_*)(r-r_*) + \beta_{R\theta}(R-R_*)(\theta-\theta_*) + \beta_{r\theta}(r-r_*)(\theta-\theta_*). \tag{3.9}$$

The second-order expansion of the potential energy surface about the saddle point is

$$V(R,r,\theta) = -\frac{1}{2}\left(M\Omega^2 - 36\mu\omega_*^2\left(\frac{r_*-r_\infty}{R_*}\right)^2 - 72\frac{V_0\theta_*^2}{R_*^2}\right)(R-R_*)^2 + \frac{1}{2}\mu\omega_*^2(r-r_*)^2 + V_0(\theta-\theta_*)^2 + 6\mu\omega_*^2\left(\frac{r_*-r_\infty}{R_*}\right)(R-R_*)(r-r_*) + 12\frac{V_0\theta_*}{R_*}(R-R_*)(\theta-\theta_*) + \cdots. \tag{3.10}$$

The analysis of the first bracket of the right-hand side of Eq. (3.10) shows that the force constant of the unstable mode is modified by curvature effects and that the frequency Ω defined in Eq. (3.2) is a zeroth-order quantity. The bracketed quantity must be positive and this introduces a constraint on the parameters of the model.

Clearly, not all reactive processes can be studied with this Hamiltonian. Results derived for the strongly asymmetric steepest-descent paths considered here would probably not be valid for smoother reaction profiles found, e.g., in isomerization reactions of rare gas clusters.[24] Nevertheless, we believe it to be realistic enough to identify general trends in short-time dynamics in many cases.

IV. THE CENTRAL REACTIVE TRAJECTORY

We start with the central reactive trajectory, corresponding to the set of initial conditions defined in Eq. (2.10). The internal energy is then partitioned into translational and vibrational kinetic energy only. As a result, the value of the modulus of the vibrational momentum is determined by the magnitude of P_{R*},

$$P_r = \pm\sqrt{2\mu}\sqrt{E - \frac{P_{R_*}^2}{2M}}. \tag{4.1}$$

As previously seen in Sec. II, the quadratic coefficient c_2 is automatically equal to zero.

Now, evaluate the cubic coefficient, given by Eq. (2.11) in order to determine under which conditions it is indeed positive,

$$c_3 = \frac{1}{M^2}\left(\left(M\Omega^2 - 36\mu\omega_*^2\left(\frac{r_*-r_\infty}{R_*}\right)^2 - 72\frac{V_0\theta_*^2}{R_*^2}\right)P_{R_*} - 6M\omega_*^2\left(\frac{r_*-r_\infty}{R_*}\right)P_r\right). \tag{4.2}$$

When compared with Eq. (3.10), the first of the bracketed expressions is seen to be proportional to the modulus of the imaginary frequency of the TS and is therefore necessarily positive. This means that a high value of the translational momentum P_{R^*} is always beneficial to reactivity. By contrast, a nonzero value of the vibrational momentum is beneficial only if the product $(r_* - r_\infty)P_r$ is negative, i.e., if the sign of P_r is properly coordinated with the equilibrium distances of the diatomic fragment in the TS and at its asymptotic value, which is compatible with Eq. (2.12).

Little information that would be workable in practice can be found in the expression of the quartic coefficient c_4, except that it consists of a sum of small terms of undecidable sign having dimension M^{-3}.

Now, consider the leading terms of the quintic coefficient c_5,

$$c_5 = \frac{1}{M^3}\left(\left(\left(M\Omega^2 - 36\mu\omega_*^2\left(\frac{r_*-r_\infty}{R_*}\right)^2 - 72\frac{V_0\theta_*^2}{R_*^2}\right)^2 + 36M\mu\omega_*^4\left(\frac{r_*-r_\infty}{R_*}\right)^2 + \left(12\frac{V_0\theta_*}{R_*^2}\right)^2\left(1+\frac{MR_*^2}{\mu r_*^2}\right)\right)P_{R_*} + 6M\omega_*^2\left(\frac{r_*-r_\infty}{R_*}\right)\left(M\left(\omega_*^2-\Omega^2\right) + 36\mu\omega_*^2\left(\frac{r_*-r_\infty}{R_*}\right)^2 + 72\frac{V_0\theta_*^2}{R_*^2}\right)P_r\right). \tag{4.3}$$

As expected, the coefficient of P_{R*} consists of a sum of squares. Thus, a high value of the translational momentum is automatically beneficial to reactivity. However, the situation concerning the role of P_r is different for the cubic and quintic coefficients and may lead to contradictory requirements, as already predicted in Sec. II. As shown by a comparison between Eqs. (4.2) and (4.3), the conditions subject to which an increase of the vibrational momentum increases reactivity are opposite for the cubic and quintic terms: for the latter, the product $(r_* - r_\infty) P_r$ must be positive (at least in the common case where $\omega_* > \Omega$).

Summarizing, energy flow into the translational momentum invariably stimulates reactivity. On the other hand, energy deposition into the vibrational momentum increases one coefficient and reduces the other: what is gained on one side is lost on the other and the net result is unpredictable. However, it is easily understood that for low values of the initial translational momentum P_{R^*}, the reactivity will be determined by the initial vibrational momentum P_r. In that case, the appropriate sign that should be given to it should be derived from the expression of the coefficient c_3, i.e., from the second term of the right hand side of Eq. (4.2), because if c_1 is very small with $c_2 = 0$, then $c_3 > 0$ is a necessary (but not sufficient) reactivity condition.

V. REACTIVE CYLINDERS IN PHASE SPACE

Let us get back to our main problem. What happens when the trajectory is started with the set of initial conditions $\{R_*, P_{R_*}, r_* + \delta r, P_r, \theta_* + \delta\theta, P_\theta\}$?

In addition to the TST tenet $c_1 = P_{R_*}/M > 0$, the second essential requirement for a trajectory to be reactive is that its initial conditions should reduce the quadratic term to zero. The evaluation of Eq. (2.9) leads to a fairly complicated expression and a series expansion is necessary to derive a workable formula. The simplest expression of an initial condition that reduces the magnitude of the quadratic coefficient c_2 to a very small value is found to be

$$\delta r = \left(\mu\omega_*^2 (r_* - r_\infty)\right)^{-1} \left(\frac{P_\theta^2}{6MR_*^2} + V_0\delta\theta^2 - 2V_0\theta_*\delta\theta \right). \tag{5.1}$$

Note that the influence of P_θ is reduced by the magnitude of nuclear masses. In the limiting case of a very loose TS, i.e., when $r_* = r_\infty$, with $\omega_* = \omega_\infty$ and $\theta_* \neq 0$, the appropriate initial condition becomes

$$\delta\theta = \frac{P_\theta^2}{12MR_*^2V_0\theta_*}. \tag{5.1a}$$

If the TS is totally loose, i.e., when $r_* = r_\infty$, $\omega_* = \omega_\infty$, and $\theta_* = 0$, then the only solution is to set δr, $\delta\theta$, and P_θ all three equal to zero.

Now, evaluate the cubic coefficient for an adjacent trajectory when the zero-acceleration condition is satisfied, i.e., when δr is given by Eq. (5.1). One finds that the value of the cubic coefficient c_3 is still given by Eq. (4.2) plus additional terms, which we denote as Δc_3, with

$$\Delta c_3 = \frac{2}{MR_*}\left(\frac{6}{M}\left(19\frac{V_0\theta_*}{R_*} - \beta_{R\theta} \right)\delta\theta P_{R_*} - 3\frac{\beta_{r\theta}}{\mu}\delta\theta P_r - 6\frac{V_0\theta_*}{I_*}P_\theta + 2\left(\frac{2V_0}{I_*} + \frac{V_0}{\mu r_*^2} - 3\frac{\beta_{\theta\theta}}{I_*} \right)\delta\theta P_\theta \right). \tag{5.2}$$

We note that trajectories that depart from the central reactive one are not necessarily less reactive if the signs of the initial momenta and of $\delta\theta$ are properly chosen to make Δc_3 positive. The same is true for higher-order terms (c_5 and higher). A compromise can be sought among the various odd-order coefficients, which should lead to the formation of a bundle of related trajectories that form a so-called "reactive cylinder" (or a "conduit") in phase space.

This concept that has a long history. It was first introduced by DeLeon and co-workers[25] and confirmed by Hutchinson *et al.*[21] Conduits in phase space that reacting trajectories must follow have been calculated in normal-form coordinates by Wiggins,[12] Komatsuzaki,[11] and their co-workers. Trajectory calculations done by Fair *et al.*[21] and by Waalkens *et al.*,[12] offer spectacular illustrations of the concept of reactive cylinders in phase space.

Finally, the concept of bundles of trajectories that form a flux tube is found to remain valid in a quantum-mechanical formulation[26] that will be discussed in Sec. VIII.

VI. NUMERICAL TRAJECTORY CALCULATIONS

We now wish to present a numerical illustration of the subspace of initial conditions that generate reactive trajectories.

Active phase space graphics were determined in the following way. There are six degrees of freedom in our problem. However, useful information about the reactive phase space can be presented in low-dimensional graphs. The dimensionality can be reduced by fixing R at R_*, by eliminating δr via Eq. (5.1), and by assigning a particular value to P_{R^*}. Then, at each value of the latter momentum, the reactive subspace can be studied in a three dimensional space ($\delta\theta$, P_θ, P_r) enclosed in a parallelepiped box whose apices are fixed at the maximum possible value for these three degrees of freedom, i.e., $\pm \arcsin\left[V_0^{-1/2}\left(E - P_{R_*}^2/2M\right)^{1/2}\right]$, $\pm(2I_*)^{1/2}\left(E - P_{R_*}^2/2M\right)^{1/2}$, and $\pm(2\mu)^{1/2}\left(E - P_{R_*}^2/2M\right)^{1/2}$.

At each chosen value of the translational momentum P_{R^*}, the locus of reactive conditions is given as a sequence of cuts at particular values of the vibrational momentum P_r.

As indicated in Sec. IV, a high value of the translational momentum P_{R*} invariably stimulates reactivity. When it is low, energy deposition into the vibrational momentum P_r leads to effects that are difficult to predict. To investigate this point, ranges of values of these momenta were considered.

Inspection of Eqs. (4.2), (4.3), (5.1), and (5.2) shows that the equations that control the dynamics considerably simplify when $\theta_* = 0$. Therefore, collinear and bent TSs will be studied separately.

In all of the graphics to be presented shortly, the total internal energy has been fixed at a value of 1 kcal/mol above the saddle point.

A. Collinear TSs

We take the example of the reaction $H_2 + Cl \rightarrow H\cdots H\cdots Cl \rightarrow H + HCl$, whose *ab initio* potential energy surface has been calculated by Bian and Werner.[27] The values of the coupling constants β_{ij} that appear in the expression of the three-body interaction term [Eq. (3.9)] have been chosen to

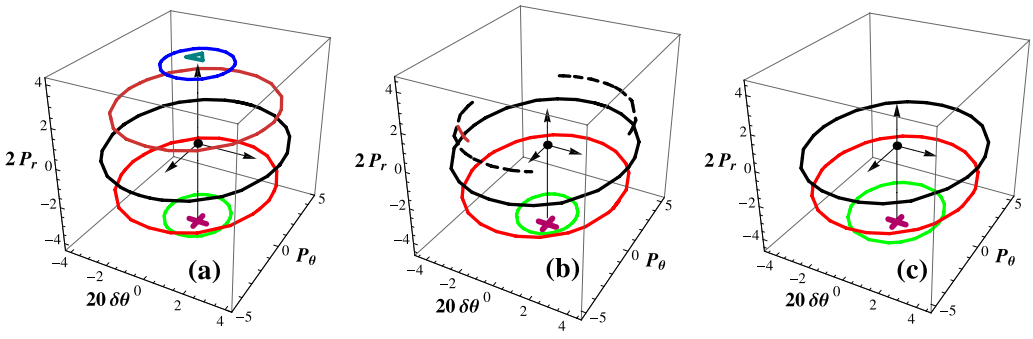

FIG. 1. Locus of initial conditions leading to reactive trajectories plotted in space ($\delta\theta$, P_θ, P_r) for the HHCl → H + Cl reaction, represented as a sequence of cuts at specific values of P_r for three values of the initial translational momentum P_{R^*}. Left graph (a): P_{R^*} = 1 a.u., close to the equipartition value. Middle graph (b): P_{R^*} = 0.25 a.u. Right (c): P_{R^*} = 0.1 a.u. Color code for the cuts: green: $P_r = -2$ a.u.; red: $P_r = -1$ a.u.; black: $P_r = 0$; brown: $P_r = +1$ a.u.; blue: $P_r = +2$ a.u.; dashed: $P_r = +0.75$ a.u. Turquoise triangle: P_r fixed at its maximum positive value. Purple cross: P_r fixed at its most negative value. Total internal energy = 1 kcal/mol.

generate the van der Waals well that appears in the exit channel of the potential energy surface.

Three values of the translational momentum have been considered and the results are presented in Fig. 1.

In Fig. 1(a), the translational momentum has been given the value P_{R*} = 1 a.u., close to that obtained when the internal energy is equipartitioned among five degrees of freedom, i.e., $P_{R_*} = \sqrt{2ME/5}$ = 1.06 a.u. The turquoise triangle and the purple cross denote the two central reactive trajectories, with initial conditions $\delta\theta = 0$, $P_\theta = 0$, and P_r fixed at its two maximum values given by Eq. (4.1). Classical trajectories were calculated to verify that both are reactive.

As stated in Sec. V, families of reactive trajectories can also be found with properly chosen nonzero values of $\delta\theta$ and P_θ. For each value of P_r, a sufficient number of trajectories were calculated by numerical integration of Hamilton's equations up to very large fragment separations. In each case, these numerical trajectories were all confirmed to be reactive. They are represented in the graph as a sequence of cuts at particular values of the vibrational momentum P_r. When considered together, they form a reactive locus that has the shape of a three-dimensional ellipsoidal surface.

The ellipsoidal shape of the locus of reactive initial conditions can be understood by formulating the energy conservation condition at $R = R_*$ and at a value of r determined by the reactivity criterion given by Eq. (5.1). The result is then Taylor expanded in the two variables $\delta\theta$ and P_θ. One gets

$$E - \frac{P_{R_*}^2}{2M} - \frac{P_r^2}{2\mu} = V_0\delta\theta^2 + \frac{P_\theta^2}{2I_*} + \text{h.o.t.}, \qquad (6.1)$$

where the higher-order terms involve $\delta\theta^2 P_\theta{}^2$. Numerical calculations show them to be quite negligible. Thus, at fixed values of P_{R*} and P_r, Eq. (6.1) is that of an ellipse.

In short, at values of P_{R^*} close to or higher than energy equipartition, Eq. (5.1) provides a reliable way to select reactive trajectories and constitutes a necessary and sufficient reactivity criterion. This is unfortunately no longer the case at lower values of the translational momentum, as shown by the next two graphs.

Part (b) of Fig. 1 describes the situation when the initial translational momentum is equal to one-fourth of the equipartitioned value, i.e., to P_{R*} = 0.25 a.u. The purple cross corresponds to the central reactive trajectory with $\delta\theta = 0$, $P_\theta = 0$, $P_r = -(2\mu)^{1/2}\left(E - (0.25)^2/2M\right)^{1/2}$. The same zero values for $\delta\theta$ and P_θ when the positive sign is chosen for P_r generate a recrossing trajectory because reactivity is then no longer favored by a high value of the translational momentum. Moreover, for nonzero values of $\delta\theta$ and P_θ, the ellipsoid is now incomplete. Its lower part, corresponding to negative values of P_r still subsists. For weakly positive values of P_r, the locus of reactive initial conditions still forms a complete ellipse. However, as P_r is still increased, the reactive locus is no longer a closed curve but splits into two open loops, drawn with a dashed line. Still higher, only a brief segment of reactive initial conditions (represented in brown) subsists. Trajectories are reactive if they are started within the open loops. They recross if started beyond its extremities.

Clearly, at low values of P_{R*}, reactivity is controlled by the sign of the vibrational momentum. It is maintained for negative values of P_r, but positive values are discriminated against. This observation can be accounted for by noting that $r_* > r_\infty$ in the activated complex H ⋯ H ⋯ Cl. Therefore, the product $-(r_* - r_\infty)\,P_r$ that appears in second bracketed term of the right hand side of Eq. (4.2) increases the magnitude of the coefficient c_3 for negative values of P_r only.

Part (c) of Fig. 1 corresponds to P_{R*} = 0.1 a.u.; the energy stored in the translational momentum is thus one hundredth of the equipartitioned value. No trajectory starting with a positive value of P_r can be reactive. The black curve, corresponding to a zero value of P_r, is the upper limit.

In summary, three conclusions emerge. (i) Trajectories that strongly deviate from the central one defined in Sec. II C are observed to be reactive. (ii) Equation (5.1) eliminates one degree of freedom from the reactive phase space. (iii) At high values of P_{R^*}, Eq. (5.1) is a necessary and sufficient reactivity criterion. However, it proves necessary to discard some particular points in that part of phase space corresponding to low values of P_{R^*}.

The locus of reactive trajectories in phase space is thus highly specific. Altogether, only a small fraction of all possible initial conditions generate truly reactive trajectories. This result had already been established by Waalkens *et al.*,[12,28] who concluded that reactive trajectories do not at all explore the energy surface ergodically and issued a warning against

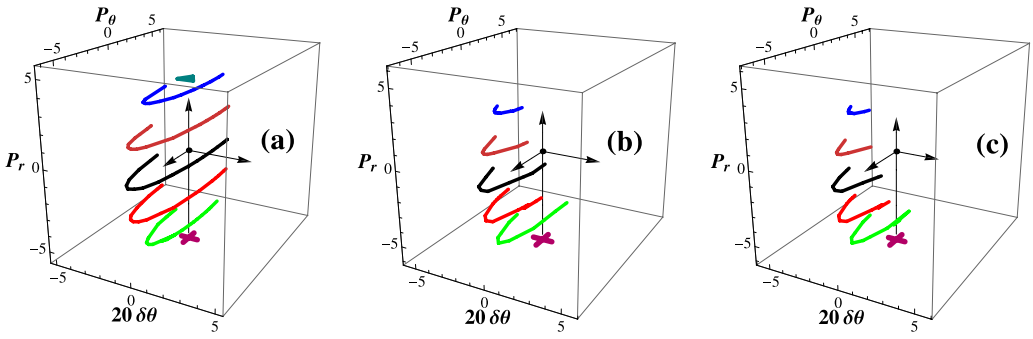

FIG. 2. Locus of initial conditions leading to reactive trajectories plotted in space ($\delta\theta$, P_θ, P_r) for the HCO → H + CO reaction, represented as a sequence of cuts at specific values of P_r for three values of the initial translational momentum P_{R^*}. Left graph (a): P_{R^*} = 1 a.u., close to the equipartition value. Middle graph (b): P_{R^*} = 0.25 a.u. Right (c): P_{R^*} = 0.1 a.u. Color code for the cuts: green: $P_r = -4$ a.u.; red: $P_r = -2$ a.u.; black: $P_r = 0$; brown: $P_r = +2$ a.u.; blue: $P_r = +4$ a.u. Turquoise triangle: P_r fixed at its maximum positive value. Purple cross: P_r fixed at its most negative value. Total internal energy = 1 kcal/mol.

the use of the ergodicity assumption in statistical theories of reactivity.

B. Bent TSs

The chosen reaction is HCO → H + HCO, whose *ab initio* potential energy surface (characterized by an angle $\theta_* = 74°$) has been determined by Song *et al.*[29] The vibrational frequencies of the TS have been calculated by Cho *et al.*[30] Here again, r_* is found to be larger than r_∞, so that reactivity is expected to be favored by negative values of P_r.

Here again, three values of the translational momentum were considered, equal to 1, 0.25, and 0.1 a.u. The value $P_{R^*} = 1$ a.u. is again close to that corresponding to energy equipartition, i.e., $P_{R_*} = \sqrt{2ME/5} = 1.06$. As shown in Fig. 2, trajectories are found to be reactive for both positive and negative values of P_r. However, the loci of reactive initial conditions are no longer closed curves: they form open loops that end up when the trajectory recrosses. The central reactive trajectory with initial conditions $\delta\theta = 0$, $P_\theta = 0$, and $P_r = -(2\mu)^{1/2}\left(E - P_{R_*}^2/2M\right)^{1/2}$, represented by a purple cross in Fig. 2, is found to be reactive for all values of P_{R^*}. The other one, with a positive sign for P_r, represented by a turquoise triangle, shows up only at high values of P_{R^*}.

Clearly, positive values of P_θ are discriminated against. This observation can be accounted for by noting the presence of the term $-6V_0\theta_* P_\theta/I_*$ in Eq. (5.2), which increases the magnitude of the cubic coefficient when P_θ is negative and which curbs reactivity when it is positive.

The shape of the locus of reactive initial conditions can be rationalized as previously done for collinear TSs. The energy conservation condition is now

$$E - \frac{P_{R_*}^2}{2M} - \frac{P_r^2}{2\mu} = V_0\left(1 + \frac{2V_0\theta_*^2}{\mu\omega_*^2(r_* - r_\infty)^2}\right)\delta\theta^2 + \frac{P_\theta^2}{2I_*} + \text{h.o.t.}, \tag{6.2}$$

where the higher-order terms are now cubic, involving $\delta\theta^3$ and $\delta\theta P_\theta^2$. They are no longer negligible and somewhat deform the loci. However, the most conspicuous effect results from the presence of the additional second term in the bracket of Eq. (6.2), which considerably increases the length of the major axis of the ellipse. Altogether, the locus may be described as roughly elliptical, with a large eccentricity resulting from a very substantial elongation in the direction of the P_θ axis.

C. Conclusions

Summing up, the comparative study of collinear and bent TSs reveals an unquestionable influence of symmetry on reactivity. These numerical calculations indicate that the reactivity criterion expressed in Eq. (5.1), together with the TST tenet $P_{R*} > 0$, provides a pair of necessary and sufficient reactivity criteria in the particular case of collinear TSs studied at not too low values of the translational momentum P_{R^*}. If this condition is not fulfilled, then Eq. (5.1) is still useful as a necessary but nonsufficient condition. Additional restrictions operate, whose origin can be qualitatively understood but which cannot be explicitly and quantitatively formulated. For collinear TSs, the additional restriction is linked to the magnitude and especially the sign of the vibrational momentum P_r. The indeterminacy is greater for bent TSs.

VII. DISCUSSION

A. A necessary but insufficient reactivity criterion

A chemical reaction is a long history when described in terms of classical trajectories that start somewhere in phase space, happen to cross a bottleneck region, undergo post-TS dynamics, and continue on their path to infinite separation. In its basic assumption, TST attempts to relate the final issue reached at asymptotic distances to very local structural and dynamical information on the immediate neighborhood of the saddle point. How is this possible?

TST can be elegantly formulated[31–33] in terms of a characteristic function χ that contains all of the dynamics of the reaction. By definition, $\chi(\mathbf{p},\mathbf{q}) = 1$ if the classical trajectory that goes through phase space point $(\mathbf{p},\mathbf{q})$ is reactive and is equal to zero otherwise. In TST, the reactivity criterion is both unique and extremely simple: $\chi = 1$ if, when evaluated at the dividing surface, the vector $\mathbf{p}$ has a component on the normal to this surface.

In our language, this criterion reduces to the condition $c_1 > 0$, i.e., to $P_{R^*} > 0$. This requirement is, however, known to

be necessary, but not sufficient. The main result of the present work is the zero-acceleration condition ($c_2 = 0$) expressed in Eq. (5.1), which has been examined at length. It reduces the other even-order terms to a small value and ensures a positive value for the P_{R^*}—dependent part of odd-order coefficients. It should be viewed as an additional necessary but still insufficient specification of the characteristic function χ.

B. The recrossing problem

In principle, the present procedure, based as it is on Eq. (2.2), i.e., on a severely truncated short-time expansion centered on the saddle point, can only give the trajectory a good start. Furthermore, as pointed out by Hernandez *et al.*,[14] information about the reaction path is not present in classical TST. (It shows up only in its semiclassical formulation.[6,34]) Therefore, one is entitled to wonder why, at least in the numerical examples considered here, this highly local, analytical reactivity criterion proves to be adequate for selecting nonrecrossing reactive trajectories and—apart from exceptions that reveal the influence of other degrees of freedom and that can be qualitatively understood—is never contradicted by the exact numerical integration of Hamilton's equations of motion during a long lapse of time.

This conclusion should be compared with the analysis of the recrossing problem that Wiggins and co-workers[8,9,12,13,15] have carried out with great mathematical rigor. These authors describe classical reaction dynamics by a Taylor expansion about the saddle point in a set of coordinates that displays a fundamental structure in the Hamiltonian and that leads to a separation of Hamilton's equations near the saddle. We quote from them: "Global recrossing cannot be avoided.... A trajectory, after having crossed the dividing surface, has to leave the neighborhood of the dividing surface before it can possibly cross it again.... Global recrossing of any single dividing surface is an inherent property of the dynamics...."

In our formulation, recrossings are unavoidable when initial conditions do not satisfy Eq. (5.1). In addition, as amply discussed in Sec. VI, recrossings are possible for certain combinations of momenta even when this equation is satisfied. The main point to be analyzed is the essence of TST, namely, the postulated link between a highly local analysis of a very small part of phase space in the immediate vicinity of the saddle point and the exact solution of Hamilton's equations in the whole time range. We propose the following line of thought.

In Secs. II B and II C it has been argued that, once the zero-acceleration condition that will later on lead to Eq. (5.1) has been adopted, mathematical constraints appear in the sequence of Poisson brackets that persist up to a high order, irrespective of the shape of the potential energy function $V(R,r,\theta)$: the P_{R^*}—dependent part of odd-order coefficients (linear, cubic, quintic, and even higher) is necessarily positive. As a result, any energy flow into the reaction coordinate necessarily increases reactivity.

However, it was also noted that the strictness of these constraints decreases with the order of the coefficient, i.e., decreases with progress along the reaction coordinate. Understandably enough, it becomes increasingly difficult to predict the evolution as one moves away from the origin of the expansion, i.e., away from the saddle point. Further information on the shape of the potential energy surface is necessary to predict the behavior at later stages.

All this can be understood if the good start provided by the zero acceleration condition, namely, Eq. (5.1), is sufficient to reach a region where the TST model can be replaced by another one describing the motion of rotating and vibrating fragments in an asymptotic repulsive force field. A point of inflection next to the saddle point seems to be a quite natural locus for the transition between the two regimes and the presence of such a point seems to be an essential element for the success of TST. In the two examples that have been numerically studied in Sec. VI, the intrinsic reaction coordinate is characterized by a single point of inflection, which is found beyond the saddle point.

The correlation with the observed dynamics is particularly conspicuous in the bent TS case. Most of the trajectories exhibit a jolt or a plateau that is invariably found at negative times only, i.e., in the reactant part of configuration space where no inflection point is found along the intrinsic reaction coordinate. However, they all become suddenly smoothly reactive with a steadily positive gradient at positive times. The percentage of reactive trajectories that do otherwise is very small. Out of 180 trajectories calculated in the study of the bent case, only 6 were found to exhibit a jolt or a plateau at positive times: 4 when $P_{R^*} = 0.1$ a.u., 2 when $P_{R^*} = 0.25$ a.u., and none when $P_{R^*} = 1$ a.u. (close to energy equipartition). In conclusion, the presence of a point of inflection along the intrinsic reaction coordinate is seen to clearly influence the dynamics.

In the collinear case, all trajectories are found to be smoothly reactive, with a steady increase of R as time goes by. The only exceptions are found when P_{R^*} is less than the equipartition value at positive values of P_r, near the edges of the two branches of the locus of reactive trajectories (represented as a dashed line in Fig. 1(b)) and for the entire tiny segment represented in brown in Fig. 1(b). As already noted, the resulting jolts and plateaus observed in these cases are due to the adverse influence of positive values of P_r on reactivity. It would be interesting to study a case where the saddle is bracketed by two points of inflection.

If this view is correct, then TST is a valid approach, provided that the concept of a dividing region having a certain width replaces that of dividing surface. The partition between reactant and product spaces should be given a certain width,[31,32] and this width might be directly related to the distance between saddle and inflection points.

C. Perspective for the future

The present model is still at its beginning and additional work is required. Among the points we wish to examine in the future, the suggestion that one of the keys to understanding chemical reactivity might be hidden in the joint presence of a saddle followed by an inflection point, irrespective of the remainder of the potential energy surface, needs to be further developed. First, because the very concept of inflection point is not entirely clear for a multidimensional system. Second,

because the equations contained in Sections II B, II C, IV, and V should be seen as a progressive derivation of mathematical properties inherent in a saddle point as the dimensionality of the potential is increased, all the way from a one-dimensional parabola to a typical TS built up from a translational coordinate plus a conserved vibrational degree of freedom plus a transitional rotational mode. The present study stops at that point. More complicated situations have not been considered. Finally, in Sec. VIII, we present a further argument which confirms that it would be interesting to study the implications resulting from the presence of a point of inflection next to the saddle point.

However, in an ever-growing number of cases, the reaction dynamics has been shown not to be mediated by a single conventional TS. Such cases are described as non-minimum energy path reactions,[35] and roaming mechanisms.[36,37] In addition, there is currently much interest in valley-ridge inflection points, which occur when the steepest-descent path connects two TSs.[38,39] We must reserve judgment concerning such reactions.

The second point that needs elaboration is as follows. We are willing to do our best in continuing the collective effort[8–15] that aims at identifying mathematical properties inherent in the existence of a saddle point that have great impact on chemical reactivity, irrespective of the shape of the potential. An additional suggestion has been proposed here: the origin of reactivity should be traced back to the *mathematical* properties of the terms of the Taylor expansion in Eq. (2.2): namely, systematic smallness for even-order terms and large magnitude for odd-order ones. This attempt contrasts with the usual approach, which looks for *physical* features of the potential (such as intramolecular mode-mode couplings or adiabaticity of some degrees of freedom, or flatness of the saddle). However, it should be immediately realized that once a specific potential energy function has been adopted, the explicit expression of a reactivity criterion is formulated in terms of structural molecular parameters, like $R_*, \Omega, r_*, \omega_*$, or in terms of force constants if the potential is formulated as a Taylor expansion. This new appearance is more appealing, at least to chemists, but conceals the basic mathematical reasons.

In Paper I,[16] a further regularity (concerning motion coordination) was shown to be independent of the shape of the potential energy function. Efforts should be sustained to find additional examples and to formulate them in chemical language. The potential is hopefully not exhausted.

VIII. TRAJECTORIES IN QUANTUM MECHANICS

The present section has a necessarily limited scope since a quantum mechanical solution cannot be derived from strictly classical results. However, it is interesting to examine the hydrodynamic model of quantum mechanics,[26,40–45] where the concept of trajectory is reintroduced. It will emerge that, in line with arguments developed in Sec. VII, the presence of an inflection point near the saddle has an incidence on the mean motion of a wave packet.

Of course, a wave packet is a superposition of quantum states characterized by a broad range of energies and the bunch of classical trajectories must go beyond a microcanonical selection. In this approach, the evolution of the system is interpreted in terms of a flowing fluid that is approximated by a finite collection of representative particles. The wave function is put in its polar form[40–43]

$$\psi(\mathbf{x},t) = A(\mathbf{x},t)\, e^{iS(\mathbf{x},\,t)/\hbar}, \tag{8.1}$$

in which S has the dimension of an action, whereas A is the square root of a density function that has the dimension $L^{-3/2}$ in a three-dimensional case. Inserting Eq. (8.1) into the time-dependent Schrödinger equation and separating into real and imaginary parts leads to two equations.

Define a density of particles $\rho(\mathbf{x},t)$ by the equation $\rho = A^2$ and a flux of particles by $\mathbf{J} = A^2 \nabla S/m = \rho\,\mathbf{v}$. Then, the imaginary part may be brought to the form[26,40–45]

$$\partial\rho/\partial t + \nabla\cdot\mathbf{J} = 0, \tag{8.2}$$

which is the equation of continuity of the flow of the set of particles.

The real part gives[40,43,44]

$$\frac{\partial S}{\partial t} + \frac{(\nabla S)^2}{2\,m} - \frac{\hbar^2}{2\,m}\frac{\nabla^2 A}{A} + V = 0 \tag{8.3}$$

which, as pointed out by Messiah,[46] represents in the classical limit ($\hbar = 0$) the dynamical equations for these particles when subjected to the potential V. In the quantum case ($\hbar \neq 0$), the particles move according to the equation of motion,[26,40–45]

$$m(d\mathbf{v}/dt) = -\nabla\left(V + V_{qu}\right), \tag{8.4}$$

where $V(\mathbf{r})$ is the classical potential and V_{qu} is a quantum potential defined by

$$V_{qu} = \left(-\hbar^2/2\,m\right)\left(\nabla^2\rho^{1/2}/\rho^{1/2}\right). \tag{8.5}$$

The nonlocal quantum potential measures the curvature of the quantum amplitude around each point in space.[26,44] It is responsible for all typically quantum effects that characterize the evolution of a wave packet, namely, tunneling, flattening, and interferences.

This hydrodynamical formulation of quantum dynamics has been extensively applied to study the motion of wave packets on potential energy surfaces, in spite of the complexity of the quantum potential.[45] However, detailed calculations require an extensive computational effort and we now wish to show that a shortcut is available.

As emphasized by Miller,[47] suitable averages very quickly tend to wash out quantum effects. The determination of the mean motion of the wave packet is known to be much simpler than that of individual trajectories because the expectation value for the quantum force vanishes at all times.[41,43] Therefore, it is exclusively the classical potential $V(R)$ that matters in a study of the overall motion. This result is known as Ehrenfest's theorem,[41,43,46,48] which provides that expectation values of coordinates and momenta satisfy the laws of classical mechanics. However, one more condition is necessary: the average force coincides with the force at the average position only if $V(R)$ is a polynomial potential of order no higher than the second, or if the wave packet is sufficiently localized. If this is not the case, then a corrective term appears.

To clarify matters, consider the one-dimensional potential characterized by a saddle point previously studied. The equation of motion of a particle moving under the influence of the inverse Lennard-Jones potential given by Eq. (3.2) is[48,49]

$$\frac{d}{dt}\langle P_R\rangle = -\frac{\partial H(\langle P_R\rangle, \langle R\rangle)}{\partial \langle R\rangle}(1+\Phi(R)). \quad (8.6)$$

The center of the wave packet moves classically where the corrective function Φ vanishes.

The core of the present paper is a procedure for selecting a bundle of classical collimated reactive trajectories by discarding those that go astray in various directions. When one now turns to quantum mechanics, one sees that the center of the wave packet can be expected to follow classical equations during the early stages of its evolution for two reasons. First, because the function Φ vanishes at the saddle point ($R = R_*$) since the wave packet feels a harmonic potential. The corrective function also vanishes at the point of inflection $\left(R = (13/7)^{1/6} R_* = 1.09\, R_*\right)$ because the potential is then linear. In the short range between these two points, the motion remains classical because the potential can safely be expected to be expressed as a linear combination of linear and quadratic terms. The second reason is that the selection of a bundle of reactive trajectories amounts to reducing the size of the spatial region of initial conditions and therefore the width of the wave packet in coordinate space.

At larger values of R, an approximation of the corrective function is available,[48,49]

$$\Phi(R) \approx \frac{d^2}{2}\left|\left(\partial^3 V/\partial R^3\right)/\left(\partial V/\partial R\right)\right|, \quad (8.7)$$

where d is the diameter of the packet. An explicit expression of the function Φ for the potential specified in Eq. (3.2) is, putting $\rho = R/R_*$,

$$\Phi(\rho) = 7\left(\frac{d}{R_*}\right)^2\left(\frac{4\rho^6 - 13}{\rho^8 - \rho^2}\right). \quad (8.8)$$

This function is equal to zero at the short distance $\rho = 1.217$ and vanishes asymptotically. It has its maximum at $\rho = 1.484$, where it is equal to $9.76\,(d/R_*)^2$.

The final conclusion is that the motion of the center of the wave packet is determined by classical equations of motion during its entire evolution if $9.76\,(d/R_*)^2 \ll 1$, i.e., if

$$d \ll 0.32\, R_*. \quad (8.9)$$

A study of the influence of the energy is possible via an alternative formulation involving the de Broglie wavelength.[48] The motion of the center of the wave packet will be classical during its entire evolution if

$$\frac{\hbar}{\sqrt{2M}\sqrt{E - V(R)}} \ll 0.32\, R_*. \quad (8.10)$$

It is a known fact that classical mechanics cannot be accurate at very low energies in spite of the heaviness of nuclear masses. Nevertheless, the previous analysis suggests that the rules that have been derived to generate reactive trajectories in classical mechanics would also be useful to build up a reactive wave packet.

ACKNOWLEDGMENTS

It is a pleasure to thank Professor Bernard Leyh, Professor Michèle Desouter-Lecomte, and Professor Roland Lefebvre for helpful discussions and comments.

[1]E. Wigner, Trans. Faraday Soc. **34**, 29 (1938).
[2]B. C. Garrett and D. G. Truhlar, in *Theory and Applications of Computational Chemistry: The First Forty Years*, edited by C. Dykstra, G. Frenking, K. S. Kim, and G. E. Scuseria (Elsevier, 2005), pp. 67–87.
[3]E. Pollak and P. Pechukas, J. Chem. Phys. **69**, 1218 (1978).
[4]M. J. Davis and S. K. Gray, J. Chem. Phys. **84**, 5389 (1986).
[5]W. H. Miller, Faraday Discuss. Chem. Soc. **62**, 40 (1977).
[6]R. Hernandez and W. H. Miller, Chem. Phys. Lett. **214**, 129 (1993).
[7]S. Keshavamurthy and W. H. Miller, Chem. Phys. Lett. **205**, 96 (1993).
[8]S. Wiggins, L. Wiesenfeld, C. Jaffé, and T. Uzer, Phys. Rev. Lett. **86**, 5478 (2001).
[9]T. Uzer, C. Jaffé, J. Palacian, P. Yanguas, and S. Wiggins, Nonlinearity **21**, 957 (2002).
[10]T. Komatsuzaki and R. S. Berry, Adv. Chem. Phys. **123**, 79 (2002).
[11]C. B. Li, Y. Matsunaga, M. Toda, and T. Komatsuzaki, J. Chem. Phys. **123**, 184301 (2005).
[12]H. Waalkens, A. Burbanks, and S. Wiggins, J. Chem. Phys. **121**, 6207 (2004).
[13]H. Waalkens, R. Schubert, and S. Wiggins, Nonlinearity **21**, R1 (2008).
[14]R. Hernandez, T. Uzer, and T. Bartsch, Chem. Phys. **370**, 270 (2010).
[15]A. Goussev, R. Schubert, H. Waalkens, and S. Wiggins, Adv. Quantum Chem. **60**, 269 (2010).
[16]J. C. Lorquet, J. Chem. Phys. **140**, 134303 (2014); Erratum, **140**, 169902 (2014).
[17]J. C. Lorquet, J. Chem. Phys. **140**, 134304 (2014).
[18]H. Goldstein, C. Poole, and J. Safko, *Classical Mechanics* (Addison Wesley, San Francisco, 2002).
[19]W. H. Miller, J. Chem. Phys. **53**, 1949 (1970).
[20]N. Smith, J. Chem. Phys. **85**, 1987 (1986).
[21]J. R. Fair, K. R. Wright, and J. S. Hutchinson, J. Phys. Chem. **99**, 14707 (1995).
[22]G. Simons, R. G. Parr, and J. M. Finlan, J. Chem. Phys. **59**, 3229 (1973).
[23]J. N. Murrell, S. Carter, S. C. Farandos, P. Huxley, and A. J. C. Varandas, *Molecular Potential Energy Functions* (Wiley, Chichester, 1984).
[24]R. J. Hinde, R. S. Berry, and D. J. Wales, J. Chem. Phys. **96**, 1376 (1992).
[25]N. DeLeon, J. Chem. Phys. **96**, 285 (1992).
[26]R. E. Wyatt, Chem. Phys. Lett. **313**, 189 (1999).
[27]W. Bian and H.-J. Werner, J. Chem. Phys. **112**, 220 (2000).
[28]H. Waalkens, A. Burbanks, and S. Wiggins, Phys. Rev. Lett. **95**, 084301 (2005).
[29]L. Song, A. van der Avoird, and G. Groenenboom, J. Phys. Chem. A **117**, 7571 (2013).
[30]S. W. Cho, W. L. Hase, and K. N. Swamy, J. Phys. Chem. **94**, 7371 (1990).
[31]W. H. Miller, Acc. Chem. Res. **9**, 306 (1976).
[32]W. H. Miller, Acc. Chem. Res. **26**, 174 (1993).
[33]P. Pechukas, in *Dynamics of Molecular Collisions, Part B*, edited by W. H. Miller (Plenum, New York, 1976), pp. 269–322.
[34]R. Hernandez, J. Chem. Phys. **101**, 9534 (1994).
[35]U. Lourderaj and W. L. Hase, J. Phys. Chem. A **113**, 2236 (2009).
[36]J. M. Bowman and B. C. Shepler, Annu. Rev. Phys. Chem. **62**, 531 (2011).
[37]F. A. L. Mauguière, P. Collins, G. S. Ezra, S. C. Farantos, and S. Wiggins, J. Chem. Phys. **140**, 134112 (2014).
[38]B. Lasorne, G. Dive, D. Lauvergnat, and M. Desouter-Lecomte, J. Chem. Phys. **118**, 5831 (2003).
[39]P. Collins, B. K. Carpenter, G. S. Ezra, and S. Wiggins, J. Chem. Phys. **139**, 154108 (2013).
[40]J. H. Weiner and Y. Partom, Phys. Rev. **187**, 1134 (1969).
[41]H. E. Wilhelm, Phys. Rev. D **1**, 2278 (1970).
[42]J. H. Weiner and A. Askar, J. Chem. Phys. **54**, 3534 (1971).
[43]P. R. Holland, *The Quantum Theory of Motion* (Cambridge University Press, New York, 1993).
[44]C. L. Lopreore and R. E. Wyatt, Phys. Rev. Lett. **82**, 5190 (1999).
[45]R. E. Wyatt, *Quantum Dynamics with Trajectories: Introduction to Quantum Hydrodynamics* (Springer, New York, 2005).
[46]A. Messiah, *Quantum Mechanics* (North-Holland, Amsterdam, 1961).
[47]W. H. Miller, J. Chem. Phys. **54**, 5386 (1971).
[48]K. Gottfried, *Quantum Mechanics* (Benjamin, New York, 1966).
[49]E. J. Heller, J. Chem. Phys. **62**, 1544 (1975).